JOURNAL OF MATERIALS SCIENCE **34** (1999) 5533–5541

Investigation of the structure parameters according to the solidification parameters for pivalic acid

E. ÇADIRLI
Niğde University, Faculty of Arts and Science, Department of Physics, Niğde, Turkey

N. MARAŞLI, B. BAYENDER, M. GÜNDÜZ
Erciyes University, Faculty of Arts and Science, Department of Physics, Kayseri, Turkey
E-mail: marasli@zirve.erciyes.edu.tr

Pivalic acid was unidirectionally solidified in a temperature gradient stage. The microstructure parameters; the primary dendrite arm spacing, λ_1, secondary dendrite arm spacing, λ_2, dendrite tip radius, R and mushy zone depth, d, were measured for five different growth rates in a constant temperature gradient, G and for five different temperature gradients in a constant growth rate, V. The depending of the microstructure parameters to the solidification parameters (V, G and GV) for pivalic acid were determined by linear regression analyze. The stability constant, σ^* was calculated by using the experimental values of R and V. The results were compared with the previous works.

1. Introduction

A dendrite structure is the most frequently observed structure when a materials is solidified. Dendritic growth may be brought out by imposing either a temperature gradient in a pure materials [1] or a solute gradient in an alloy system [2]. A dendrite structure is characterised by λ_1, λ_2, R and d (Fig. 1). For directional solidification of pure materials, the experimental variables are the imposed temperature gradient, G and growth rate, V. Therefore the microstructure parameters are controlled by the temperature gradient and growth rate. In the directional solidification, the dependency of the solidification parameters to the microstructure parameters are investigated.

While the most non-metallic materials grow with faceted morphologies a few organic materials undergo non-faceted dendritic solidification [3]. These materials have been studied as transparent analogous for metals. A thin layer of organic materials may be sandwiched between two glass slides to form a specimen cell which rests across the gap between the hot and the cold plates of a temperature gradient stage on an optical microscope (Fig. 2).

The aim of the present work is to examine the effect of solidification parameters on the microstructure parameters. In order to do this, the pivalic acid has been grown unidirectionally in a thin cell to observe the structure for five different growth rates in a constant temperature gradient and for five different temperature gradients in a constant growth rate.

2. Experimental details

In the present work, the organic material "pivalic acid" was solidified in a horizontal directional solidification apparatus to directly observe microstructure *in situ* using a transmission optical microscope. The details of the apparatus and specimen preparation given in Ref. [4]. The temperatures of the heating and cooling systems were constant during the solidification. As shown in Fig. 3, the temperature gradient at the solid-liquid interface on the specimen during the solidification was observed to be constant.

The pivalic acid was slowly melted until the solid-liquid interface passed through the second thermocouple by driving the specimen cell toward to the heating system. When the solid-liquid interface was between the second and third thermocouple (0.05 mm tick K-type), the motor was stopped and the specimen was left to reach thermal equilibrium.

3. Temperature gradient, growth rate and structure parameters

After the specimen reached the steady state conditions, the solidification was started by driving the specimen toward to cooling system by synchronous motor. When the interface was passing through to the second and first thermocouples, the solidification time between the two thermocouples and the temperatures at the points of the fixed thermocouples were recorded simultaneously with a stopwatch and a Hewlett Packard

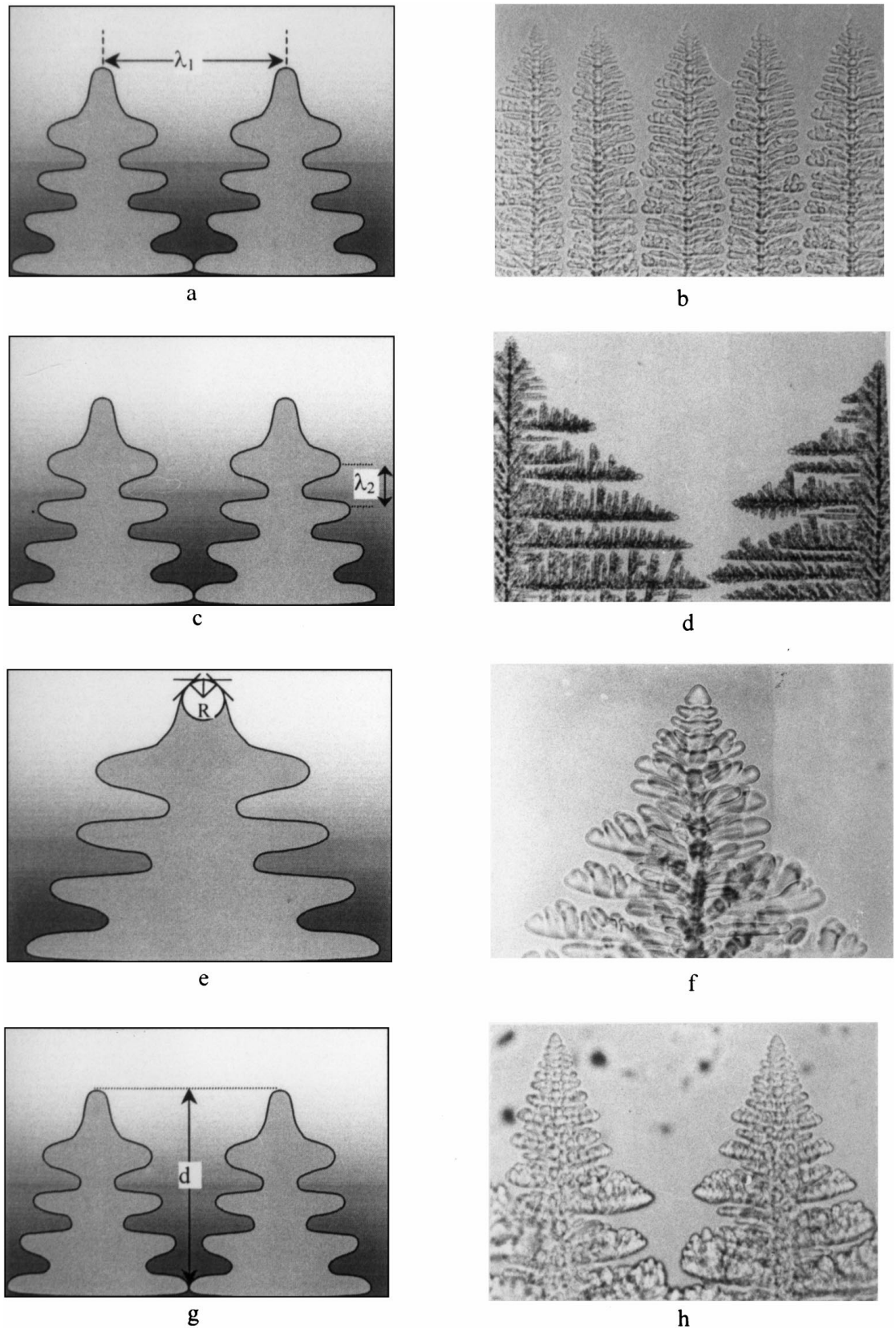

Figure 1 Definition of microstructure parameters: (a,b) schematic and photographic illustration of primary dendrite arm spacing; (c,d) schematic and photographic illustration of secondary dendrite arm spacing; (e,f) schematic and photographic illustration of dendrite tip radius; (g,h) schematic and photographic illustration of mushy zone depth.

34401 A Model multimeter, respectively. The solidification was carried out for five different growth rates in a constant temperature and for five different gradients in a constant growth rates. The photographs of the solidification microstructure were taken during the solidification. The thermocouple's positions were also photographed using 10× lens. From the photographs, the distances between the thermocouples and structure parameters were measured. Therefore the temperature gradients, growth rates and structure

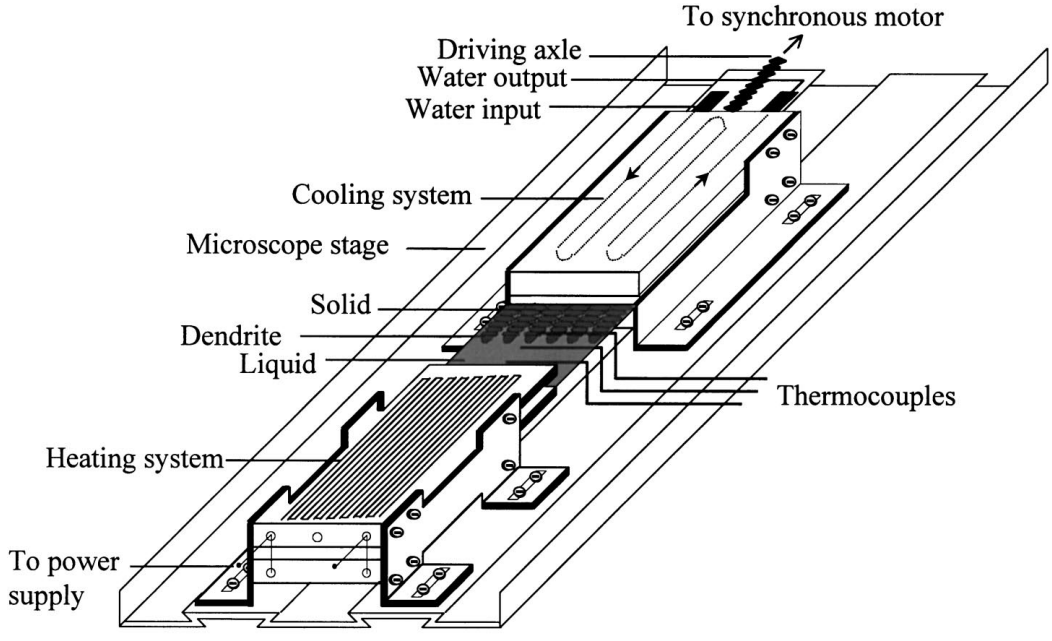

(a)

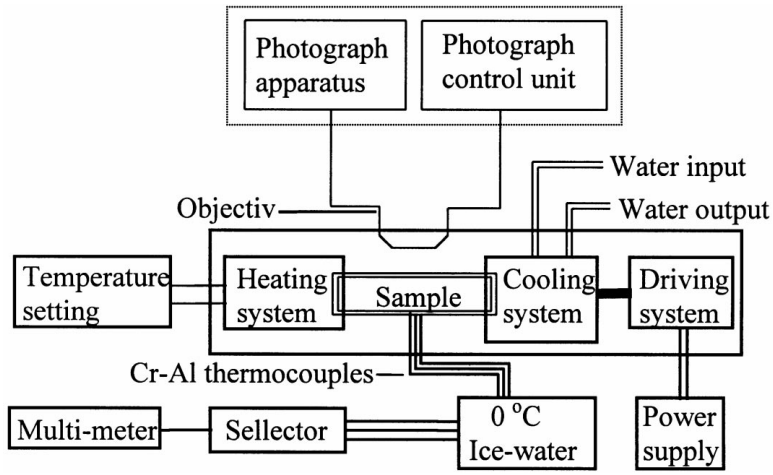

(b)

Figure 2 (a) Temperature gradient stage; (b) schematic illustration of the experimental set up.

parameters were accurately measured and are given in Table I.

4. Results and discussion

In present work, the measurements of the structure parameters; λ_1, λ_2, R and d were carried out using about 65 dendrite shapes (Figs 4 and 5). The measured structure parameters and their standard deviations are given in Table I. The relationships between microstructure parameters and the solidification parameters were obtained by linear regression analysis in three different conditions. The results are given in Table II and Figs 6–8. As can be seen from Figs 6–8, the values of

TABLE I The dependence of structure parameters (λ_1, λ_2, R, d) for different growth rates and temperature gradients

G (°C/cm)	V (cm/s) $\times 10^{-4}$	$GV \times 10^{-3}$ (°C/s)	ln G	ln V	ln GV	λ_1 (cm) $\times 10^{-4}$	λ_2 (cm) $\times 10^{-4}$	R (cm) $\times 10^{-4}$	d (cm) $\times 10^{-4}$	σ^*	ln λ_1	ln λ_2	ln R	ln d
16.38	6.7	11.07	2.79	−7.29	−4.50	209.4 ± 26.2	43.4 ± 2.4	10.2 ± 1.2	445.9 ± 43.1	0.023	−3.86	−5.43	−6.88	−3.11
16.38	11.3	18.50	2.79	−6.78	−3.98	151.6 ± 19	31.3 ± 3.4	7.7 ± 0.9	365.3 ± 51.6	0.024	−4.18	−5.76	−7.17	−3.31
16.38	19.6	32.10	2.79	−6.23	−3.43	133.0 ± 22.8	22.9 ± 2.7	5.4 ± 0.5	259.2 ± 22.5	0.029	−4.32	−6.07	−7.52	−3.65
16.38	55.2	90.41	2.79	−5.20	−2.40	108.8 ± 17.9	18.8 ± 1.6	3.6 ± 0.4	207.7 ± 27.7	0.022	−4.52	−6.27	−7.93	−3.87
16.38	85.8	140.54	2.79	−4.75	−1.96	83.3 ± 18.0	12.9 ± 0.7	2.8 ± 0.2	127.6 ± 12.1	0.024	−4.78	−6.65	−8.18	−4.36
20.50	19.6	40.18	3.02	−6.23	−3.21	122.0 ± 21.6	22.3 ± 2.4	4.9 ± 0.5	241.8 ± 22.6	—	−4.40	−6.11	−7.62	−3.72
26.27	19.6	51.48	3.26	−6.23	−2.96	113.0 ± 20.3	21.4 ± 2.5	4.5 ± 0.4	229.7 ± 20.9	—	−4.48	−6.15	−7.71	−3.77
37.75	19.6	73.99	3.63	−6.23	−2.60	104.0 ± 19.5	19.1 ± 2.1	3.9 ± 0.4	211.9 ± 19.8	—	−4.56	−6.26	−7.85	−3.85
48.64	19.6	95.33	3.88	−6.23	−2.35	86.0 ± 16.8	16.7 ± 1.8	3.2 ± 0.3	175.3 ± 17.3	—	−4.75	−6.39	−8.05	−4.04

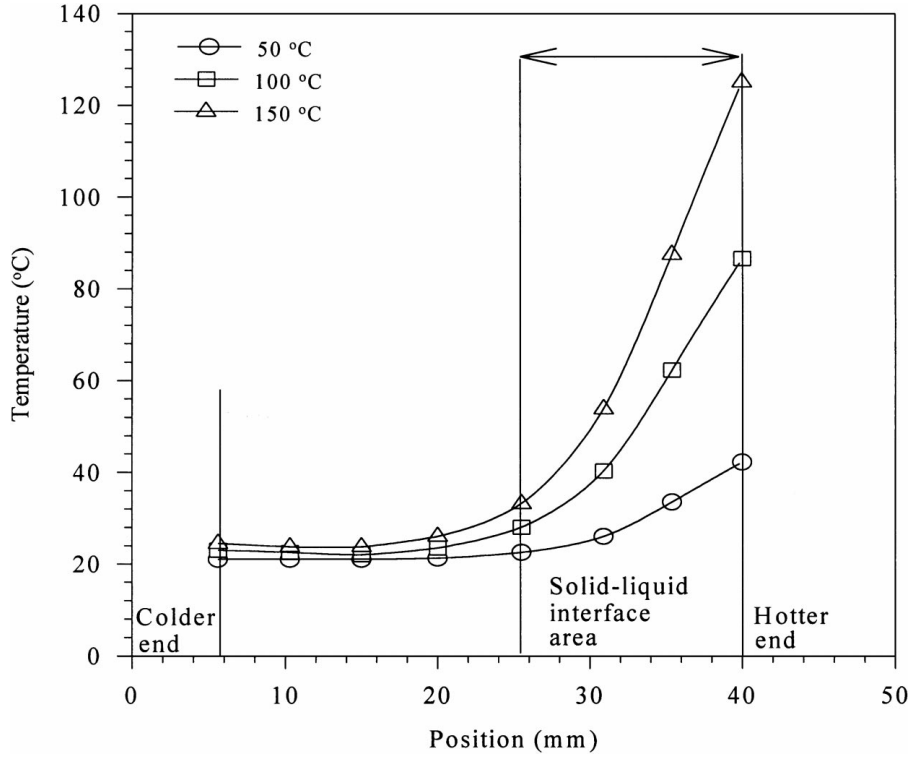

Figure 3 The plot of temperature vs. position in the sample.

TABLE II Relationships between structure parameters and solidification parameters

Solidification parameter	Structure parameter			
	λ_1	λ_2	R	d
V	$k_1 V^{-0.32}$	$k_4 V^{-0.43}$	$k_7 V^{-0.50}$	$k_{10} V^{-0.45}$
G	$k_2 G^{-0.36}$	$k_5 G^{-0.29}$	$k_8 G^{-0.46}$	$k_{11} G^{-0.33}$
GV	$k_3 (GV)^{-0.34}$	$k_6 (GV)^{-0.42}$	$k_9 (GV)^{-0.50}$	$k_{12} (GV)^{-0.44}$

k is the regression constant and r is correlation coefficient.

Constant (k)	Correlation coefficients (r)
$k_1 = 19.0 \times 10^{-4}$ cm$^{1.32}$ s$^{-0.32}$	$r_1 = -0.976$
$k_2 = 37.0 \times 10^{-3}$ cm$^{0.64}$ °C$^{0.36}$	$r_2 = -0.976$
$k_3 = 42.9 \times 10^{-4}$ cm$^{0.34}$ s$^{-0.34}$	$r_3 = -0.972$
$k_4 = 1.76 \times 10^{-4}$ cm$^{1.43}$ s$^{-0.43}$	$r_4 = -0.977$
$k_5 = 5.25 \times 10^{-3}$ cm$^{0.71}$ °C$^{0.29}$	$r_5 = -0.975$
$k_6 = 6.13 \times 10^{-4}$ cm$^{0.42}$ s$^{-0.42}$	$r_6 = -0.977$
$k_7 = 0.26 \times 10^{-4}$ cm$^{1.50}$ s$^{-0.50}$	$r_7 = -0.992$
$k_8 = 1.99 \times 10^{-3}$ cm$^{0.54}$ °C$^{0.46}$	$r_8 = -0.988$
$k_9 = 1.01 \times 10^{-4}$ cm$^{0.50}$ s$^{-0.50}$	$r_9 = -0.988$
$k_{10} = 17.0 \times 10^{-4}$ cm$^{1.45}$ s$^{-0.45}$	$r_{10} = -0.974$
$k_{11} = 65.5 \times 10^{-3}$ cm$^{0.67}$ °C$^{0.33}$	$r_{11} = -0.962$
$k_{12} = 63.0 \times 10^{-4}$ cm$^{0.44}$ s$^{-0.44}$	$r_{12} = -0.972$

λ_1, λ_2, R and d decrease exponentially as the value of G, V and GV increase.

The exponent values for λ_1, λ_2, R and d were found to be -0.32, -0.43, -0.50, and -0.45 respectively for five different growth rates in a constant temperature gradient, (16.38 °C/cm). R has the maximum exponent value and λ_1 has the minimum exponent value. The exponent values for λ_1, λ_2, R and d were found to be -0.36, -0.29, -0.46, and -0.33 respectively for five different temperature gradients in a constant growth rate, (19.6×10^{-4} cm/s). In this case, R has again the maximum exponent value but λ_2 has the minimum exponent value. The exponent values for λ_1, λ_2, R and d were found to be -0.34, -0.42, -0.50 and -0.44 respectively for increased GV values. In this case, R has the maximum exponent value and λ_1 has again the minimum exponent value.

At the all conditions, R has always the maximum exponent value. This means that tip radius decreases more rapidly than the other structure parameters as the growth rate increases. The ratios of the microstructure parameters change with the cooling rate are also given in Table III. As can be seen from Table I, the statistical error in the measurement of the structure parameters is about 10–15%. The differences between the exponent values for λ_1, λ_2, R and d given in Table II are not too large. Therefore the ratios of the microstructure parameters change with the cooling rate given in Table III seem to be constant.

A comparison of the present work with previous works is shown in Table IV. As can be seen from Table IV, the exponent values for λ_1, λ_2 and R change between -0.25 and -0.50, -0.44 and -0.58 and -0.43 and -0.53 respectively according to composition of alloys in the literature. The results obtained in present work are in good agreement with previous work [5–9].

The stability constant for pure material is given by [10, 11]

$$\sigma^* = \frac{2\alpha d_0}{V R^2} \tag{1}$$

where α is the thermal diffusivity, d_0 is the capillary length, V is the growth rate and R is the tip radius. For

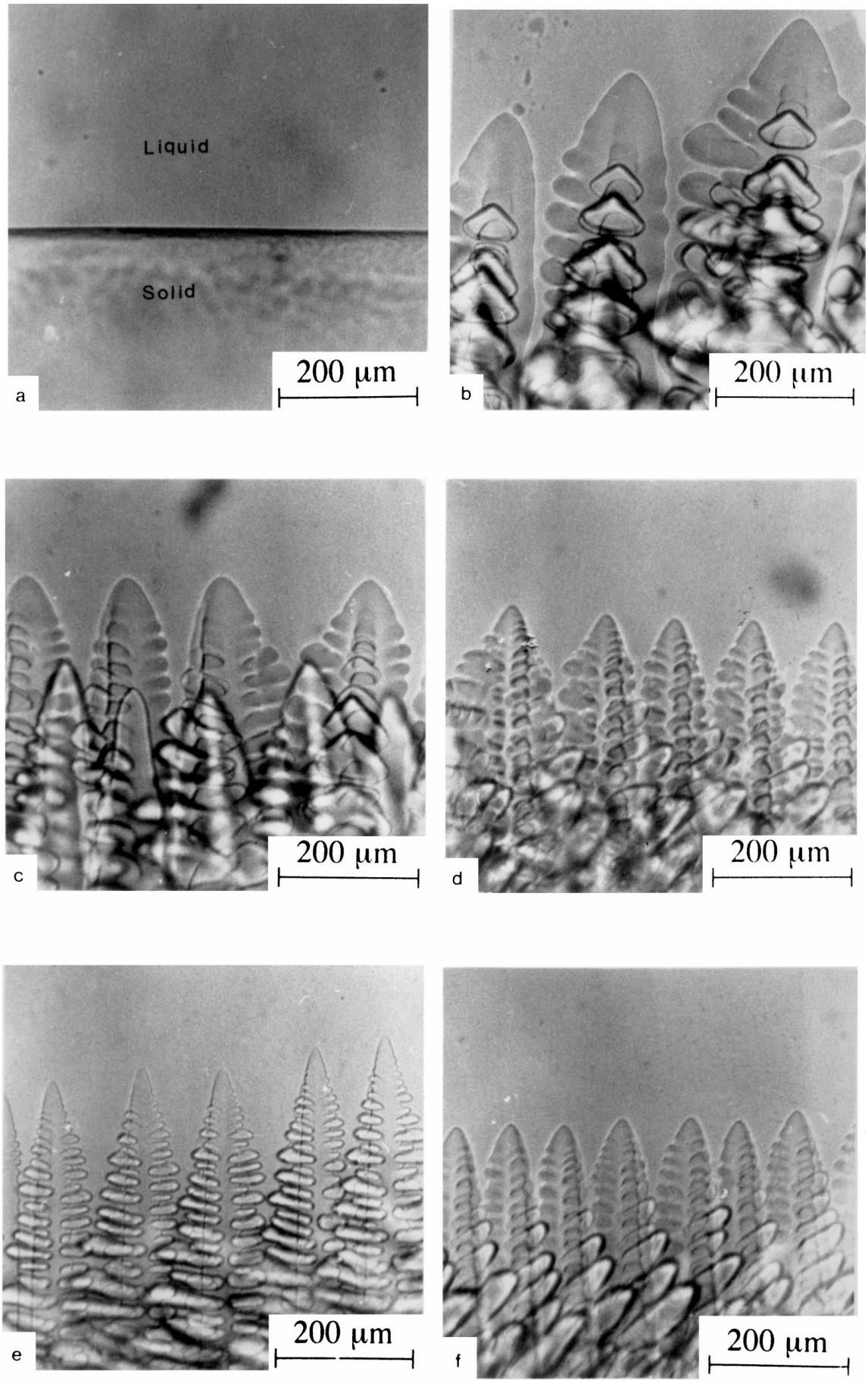

Figure 4 Solidification of pivalic acid for different growth rates at the constant temperature gradient ($G = 16.38\,^{\circ}$C/cm): (a) planar interface at equilibrium; (b) dendritic form, $V = 6.7 \times 10^{-4}$ cm/s; (c) $V = 11.3 \times 10^{-4}$ cm/s; (d) $V = 19.6 \times 10^{-4}$ cm/s; (e) $V = 56.2 \times 10^{-4}$ cm/s; (f) $V = 85.8 \times 10^{-4}$ cm/s.

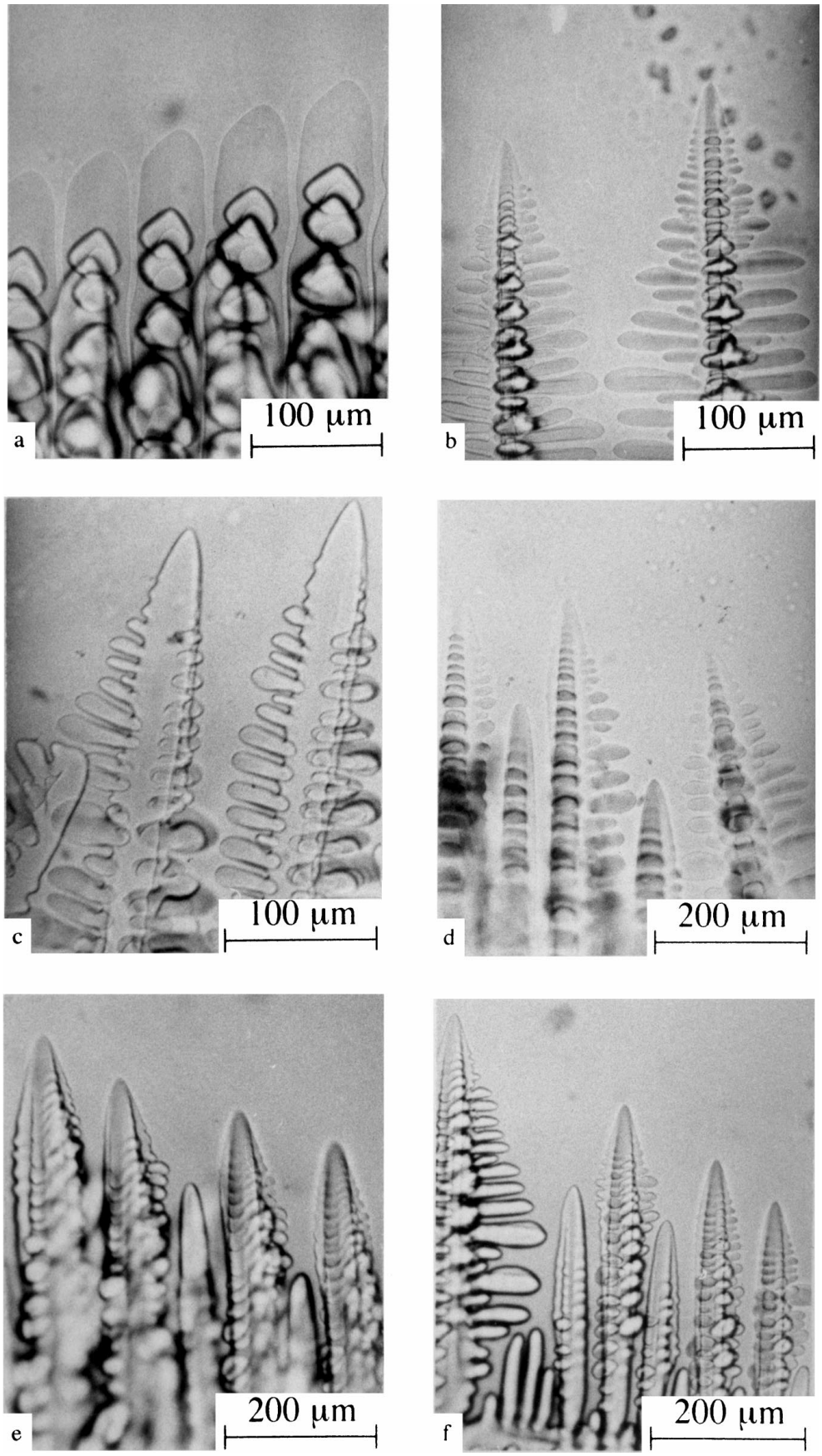

Figure 5 Solidification of pivalic acid for different temperature gradients at the constant growth rates ($V = 19.6 \times 10^{-4}$ cm/s): (a) cellular form; (b) dendritic form $G = 16.38\,^{\circ}$C/cm; (c) $G = 20.50\,^{\circ}$C/cm; (d) $G = 26.27\,^{\circ}$C/cm; (e) $G = 37.75\,^{\circ}$C/cm; (f) $G = 48.64\,^{\circ}$C/cm.

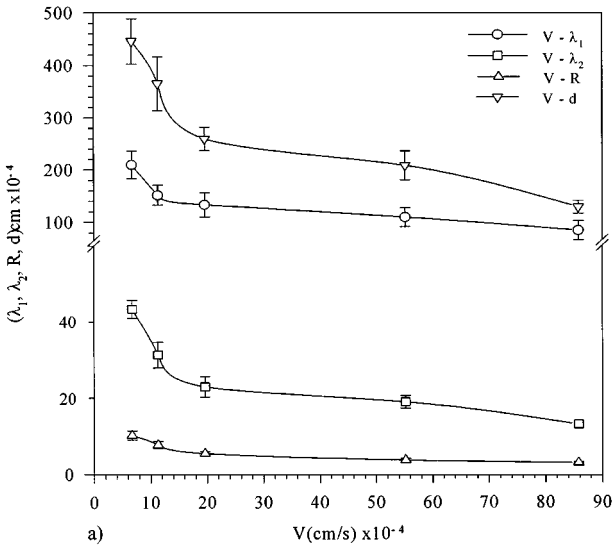

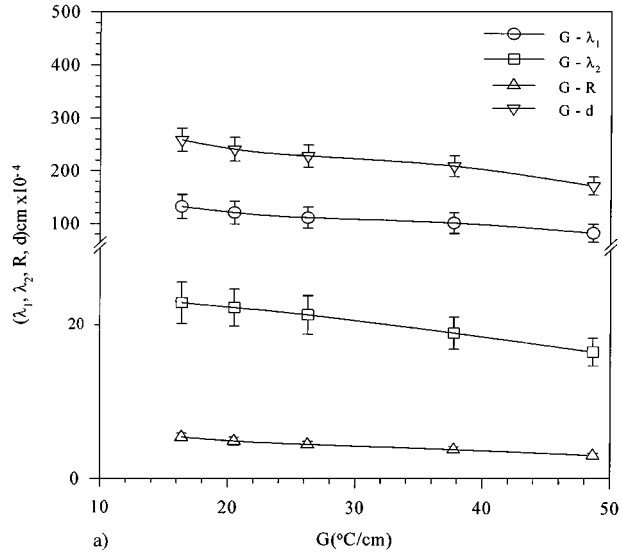

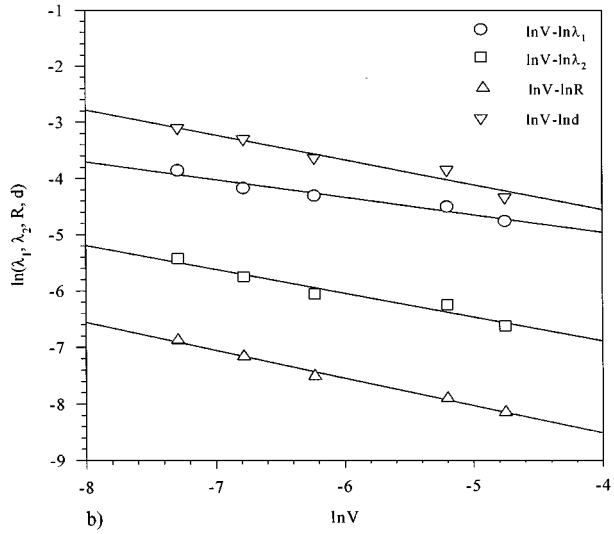

Figure 6 (a) The plot of λ_1, λ_2, R and d vs. growth rate, V; (b) The plot of ln λ_1, ln λ_2, ln R and ln d vs. ln V.

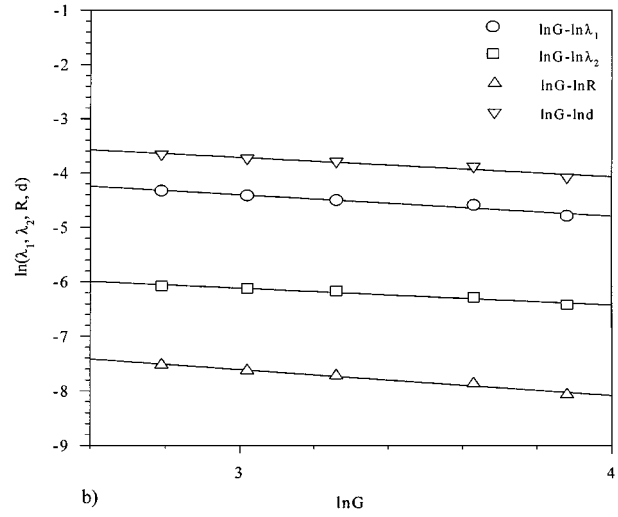

Figure 7 (a) The plot of λ_1, λ_2, R and d, vs. temperature gradient, G; (b) the plot of ln λ_1, ln λ_2, ln R and ln d vs. ln G.

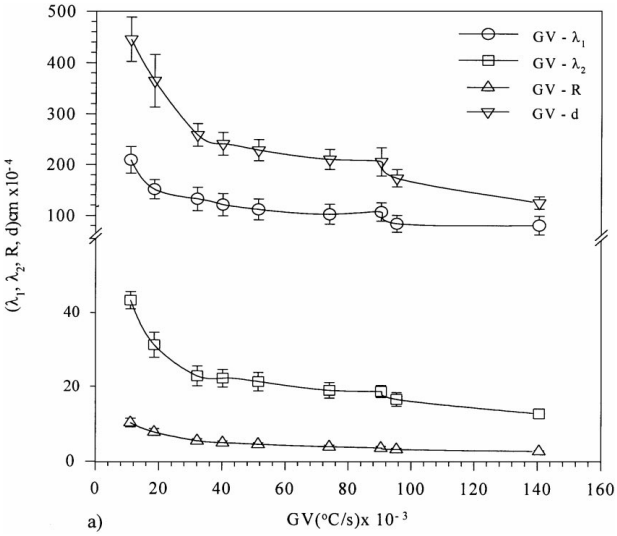

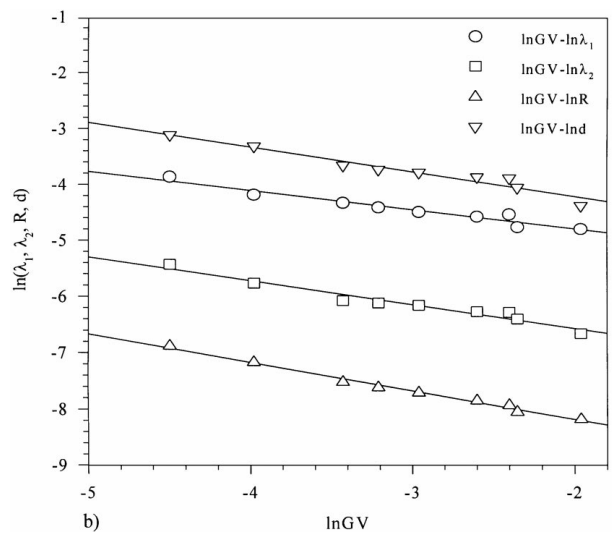

Figure 8 (a) The plot of λ_1, λ_2, R and d vs. cooling rate, GV; (b) the plot of ln λ_1, ln λ_2, ln R and ln d vs. ln GV.

TABLE III The ratio of structure parameters according to solidification parameters

G (°C/cm)	V (cm/s)$\times 10^{-4}$	GV (°C/s)$\times 10^{-3}$	λ_1/λ_2	λ_1/R	λ_1/d	d/λ_2	d/R	λ_2/R
16.38	6.7	11.07	4.82	20.52	0.47	10.27	43.71	4.25
16.38	11.3	18.50	4.84	19.68	0.42	11.67	47.44	4.06
16.38	19.6	32.10	5.80	24.62	0.51	11.31	48.00	4.24
16.38	55.2	90.41	5.78	30.22	0.52	11.04	57.69	5.22
16.38	85.8	140.54	6.45	29.75	0.65	9.89	45.57	4.60
20.50	19.6	40.18	5.47	24.89	0.50	10.84	49.34	4.55
26.27	19.6	51.48	5.28	25.11	0.49	10.73	51.04	4.76
37.75	19.6	73.99	5.44	26.66	0.49	11.09	54.33	4.88
48.64	19.6	95.33	5.15	26.87	0.49	10.50	54.78	5.22
			5.45 ± 0.49	25.37 ± 3.99	0.50 ± 0.058	10.81 ± 0.51	50.21 ± 4.36	4.64 ± 0.39

TABLE IV A comparison of the experimental results of the structure parameters (λ_1, λ_2 and R) with previous works

System	Temperature gradient (°C/cm)	Growth rate$\times 10^{-4}$ (cm/s)	Relationships	References
PVA	16.38	6.7–85.8	$\lambda_1 = kV^{-0.32}$	Present work
	16.38–48.64	19.6	$\lambda_1 = kG^{-0.36}$	”
	16.38–48.64	6.7–85.8	$\lambda_1 = k(GV)^{-0.34}$	”
	16.38	6.7–85.8	$\lambda_2 = kV^{-0.43}$	”
	16.38–48.64	19.6	$\lambda_2 = kG^{-0.29}$	”
	16.38–48.64	6.7–85.8	$\lambda_2 = k(GV)^{-0.42}$	”
	16.38	6.7–85.8	$R = kV^{-0.50}$	”
	16.38–48.64	19.6	$R = kG^{-0.46}$	”
	16.38–48.64	6.7–85.8	$R = k(GV)^{-0.50}$	”
	16.38	6.7–85.8	$d = kV^{-0.45}$	”
	16.38–48.64	19.6	$d = kG^{-0.33}$	”
	16.38–48.64	6.7–85.8	$d = k(GV)^{-0.44}$	”
KCl-5 mol % CsCl	30	13–130	$\lambda_1 \alpha V^{-0.42}$	[5]
KCl-5 mol %CsCl	30	5.2–52	$\lambda_1 \alpha V^{-0.53}$	”
SCN-13 wt % ACE	20	7.25–11.35	$\lambda_1 \alpha V^{-0.58}$	[16]
Cbr_4	70	7–100	$\lambda_1 \alpha V^{-0.55}$	[17]
SCN-25 wt % ETH	48	3–54	$\lambda_1 = 470V^{-0.42}$	[18]
SCN-2.5 wt % Benzil	16–95	56–92	$\lambda_1 = kG^{-0.50}\ V^{-0.25}$	[19]
SCN-(0.15–5)wt % ACE	38	48–225	$\lambda_1 = kG^{-0.50}\ V^{-0.25}$	”
SCN-1.4 wt % Water	62.4	140	$\lambda_1 \alpha G^{-0.50}$	[20]
Salol	54	5–75	$\lambda_1 = k(GV)^{-0.50}$	[21]
SCN-(0.001–0.004)mol % Salol	60–150	60–160	$\lambda_1 = 0.16G^{-1/3}\ V^{-1/3}\ X_0^{-1/3}$	[12]
SCN-(0.001–0.004)mol % ACE	60–150	60–160	$\lambda_1 = 0.17G^{-1/3}\ V^{-1/3}\ X_0^{-1/3}$	”
SCN-(0.001–0.004)mol % ETH	60–180	60–160	$\lambda_1 = 0.25G^{-1/3}\ V^{-1/3}\ X_0^{-1/3}$	”
SCN-4 wt % ACE	67	3.4–5.8	$\lambda_2/V = 2$	[22]
SCN-5.5 wt % ACE	—	—	$\lambda_2 \alpha V^{-0.56}$	[23]
Cbr_4-10.5 wt % C_2Cl	30	0.2–20	$\lambda_2 \alpha V^{-0.44}$	[6]
Cbr_4-7.9 wt % C_2Cl	30	0.2–20	$\lambda_2 \alpha V^{-0.45}$	”
Cbr_4-10.5 wt % C_2Cl	30	0.1–100	$R \alpha V^{-0.53}$	”
Cbr_4-7.9 wt % C_2Cl	30	0.1–100	$R \alpha V^{-0.47}$	”
PVA-0.82 wt % ETH	8.5–22.6	0.3–80	$\lambda_2 \alpha V^{-0.58}$	[7]
PVA-0.82 wt % ETH	8.5–22.6	0.3–80	$R \alpha V^{-0.54}$	”
SCN-1.3 wt % ACE	16–97	1.6–250	$\lambda_2 \alpha V^{-0.51}$	[8]
SCN-1.3 wt % ACE	16–97	1.6–250	$R \alpha V^{-0.53}$	”
SCN-2 wt % Water	24–33	0.76–105	$R \alpha V^{-0.43}$	[9]

PVA: Pivalic acid, SCN: Succinonitrile, ACE: Acetone, ETH: Ethanol.

pivalic acid, the value of d_0 is 1.11×10^{-8} cm [12] and the value of α is 0.7×10^{-3} cm^2/s [13]. The stability constant for five growth rates was calculated from Equation 1. The stability constant vs growth rate was plotted and are given in Fig. 9. As can be seen from Fig. 9, the experimental values of $\sigma^*(0)$ are very close to theoretical value.

5. Conclusions

1) The change of the microstructure parameters (λ_1, λ_2, R and d) according to the solidification parameters (V, G, GV) for pivalic acid were investigated and the relationships between them were obtained by linear regression analyze. It was seen that the values of λ_1, λ_2, R and d decreases as the values of V, G and GV increase.

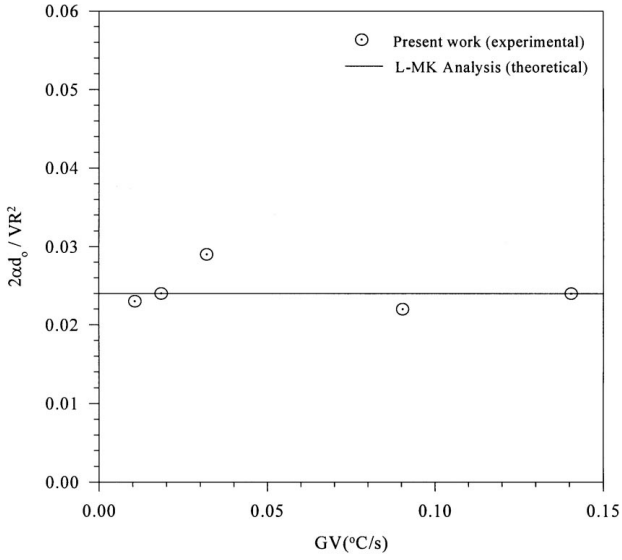

Figure 9 The plot of σ^* vs. cooling rate, GV.

2) In the present work, it was shown that the microstructure parameters can be controlled by changing of the solidification parameters. This is a very important factor for metallic materials because the mechanical properties of the metallic materials depend on the microstructure parameters [14, 15].

3) The stability constant for five different growth rates was calculated by using the experimental values of R and it was seen that the calculated values of $\sigma^*(0)$ agree with the theoretical value.

Acknowledgement

This project was supported by Erciyes University Research Foundation. Authors would like to thank Erciyes University Research Foundation for their financial support.

References

1. S. C. HUANG, PhD thesis, Materials Engineering Department, Rensselaer Polytechnic Institute, Troy, NY (1979).
2. M. CHOPRA, PhD thesis, Materials Engineering Department, Rensselaer Polytechnic Institute, Troy, NY (1984).
3. M. E. GLICKSMAN, "Solidification, American Society for Metals" (Ohio, 1971) p. 155.
4. B. BAYENDER, N. MARAŞLI, E. ÇADIRLI, H. ŞİŞMAN and M. GÜNDÜZ, *Journal of Crystal Growth* accepted for publication.
5. W. SCHMIDBAUER, T. WILKE and W. ASMUSS, *ibid.* **128** (1993) 240.
6. V. SEETHARAMAN, L. M. FABRIETTI and R. TRIVEDI, *ibid.* **20A** (1989) 2567.
7. R. TRIVEDI and J. T. MASON, *ibid.* **22A** (1991) 235.
8. H. ESAKA and W. KURZ, *J. Cryst. Growth* **72** (1985) 578.
9. C. A. CATTANEO, O. P. EVEQUOZ and H. R. BERTORELLO, *Scripta Metall.* **3/4** (1994) 461.
10. J. S. LANGER and H. MULLER-KRUMBHAAR, *Acta Metall.* **26** (1978) 1681.
11. R. TRIVEDI, *J. Cryst. Growth* **48** (1980) 93.
12. L. X. LIU and J. S. KIRKALDY, *J. Cryst. Growth* **140** (1994) 115.
13. E. R. RUBINSTEIN and M. E. GLICKSMAN, *ibid.* **112** (1991) 84.
14. P. BARTOLOTTA, J. BARRETT, T. KELLY and R. SMASLEY, *JOM.* **May** (1997) 48.
15. F. YILMAZ, R. ELLIOTT, *J. Mat. Sci.* **24** (1989) 2065.
16. S. H. HAN and R. TRIVEDI, *Acta Metall.* **42/1** (1994) 25.
17. S. DE CHEVEIGNE, C. GUTHMAN and M. M LEBRUN, *J. Cryst. Growth* **73** (1985) 242.
18. W. HUANG, X. GEYING and Y. ZHOU, *ibid.* **134** (1993) 105.
19. M. A. TAHA, *Metall. Sci.* **1** (1979) 9.
20. R. N. GRUGEL and Y.ZHOU, *Metall. Trans.* **20A** (1989) 969.
21. N. DEY and J. A SEKHAR, *Acta Metall.* **41/2** (1993) 409.
22. R. TRIVEDI and K. SOMBOONSUK, *Mat. Sci and Eng.* **65** (1984) 65.
23. K. SOMBOONSUK, J. T. MASON and R. TRIVEDI, *Metall Trans.* **15A** (1984) 967.

Received 12 August 1998
and accepted 20 April 1999